Aerospace Science and Technology 72 (2018) 502–515

Contents lists available at ScienceDirect

Aerospace Science and Technology

www.elsevier.com/locate/aescte

Rotor airfoil profile optimization for alleviating dynamic stall characteristics

Qing Wang, Qijun Zhao *

National Key Laboratory of Science and Technology on Rotorcraft Aeromechanics, Nanjing University of Aeronautics and Astronautics, Nanjing 210016, China

ARTICLE INFO

Article history:
Received 29 August 2017
Received in revised form 6 November 2017
Accepted 20 November 2017
Available online 24 November 2017

Keywords:
Rotor
Airfoil
Dynamic stall characteristics
Optimization design
RANS equations

ABSTRACT

In order to alleviate the dynamic stall characteristics of rotor airfoil, a high-efficient optimization method is established by coupling the SQP method with CFD method. Aiming at improving the optimized efficiency, a new strategy of linear search is established to avoid the disturbance of the penalty factors, and the optimal efficiency improves more than 30% compared with traditional line search method. In order to reduce the design variables, the CST method is employed to parameterize the airfoil section. All the flow solutions were computed by solving the URANS equations, coupled with the Spalart–Allmaras turbulence model. To reduce pitching moment and drag coefficient under dynamic stall condition, a new airfoil has been optimized based on the OA209 airfoil by employing the present optimal method. Due to the inhibition of leading edge vortex, the peaks of pitching moment and drag coefficient of the optimized airfoil are decreased about 75.8% and 44.2% at point 1, 44.0% and 41.4% at point 2 compared with the OA209 airfoil. Moreover, the optimized airfoil has better lift stall characteristics compared with the OA209 airfoil. In addition, by comparing the 3-D dynamic stall characteristics of rotor blade, it is demonstrated that the peaks of pitching moment coefficients and drag coefficients of optimized airfoil are smaller than those of OA209 airfoil at different blade radial stations.

1. Introduction

The rotor blades of helicopter work at serious unsteady environment due to the motions of pitching, flapping and rotation. As a result, the dynamic stall phenomenon usually happens in the retreating side under forward flight condition. The dynamic stall of rotor airfoil has significant influences on unsteady aerodynamic performances of rotor, and the phenomenon can limit the lifting capability and forward flight speed of helicopter [1,2]. As a result, it is necessary to research and control the dynamic stall of rotor airfoil.

In order to explore the mechanisms of dynamic stall characteristics of rotor airfoil, a lot of fundamental investigations have been conducted for decades, including experimental researches [3–8], theoretical analyses [9–11], and numerical simulations [12–16]. In recent years, some active control techniques have been used to control the unsteady characteristics of airfoil, such as vortex generators [17], zero-mass jets [18] and leading-edge droop [19]. However, these additional equipments used for active control would increase the weight of blade and instability of rotor control system inevitably. Therefore, it is useful and important to design new rotor airfoil to alleviate the dynamic stall characteristics.

Although many rotor airfoils are designed by experimental methods at typical steady conditions, it is difficult to accomplish airfoil design under dynamic stall condition due to the high cost of experimental method. Compared with experimental methods, the CFD method has advantages of shorter time consuming and lower cost. Therefore, airfoil design based on the numerical method under dynamic stall condition is welcomed by researchers. Mani [20] optimized a new rotor airfoil based on the SC1095 airfoil to reduce the peak pitching moment coefficient (Cm) while maintaining the baseline time-varying profile of lift coefficient (Cl). However, the maximum thickness of the optimized airfoil is 0.18, it is maybe not suitable for the rotor blade, especially for blade tip airfoil. Later, Wang and Zhao [21] design a new rotor airfoil based on the SC1095 airfoil under dynamic stall condition to alleviate the lift stall characteristics. Although the optimized airfoil has good aerodynamic stall characteristics and static aerodynamic characteristics, it lacks verification of rotor environment. The rotor airfoil usually works at complex aerodynamic environment and faces with time-varying freestream velocity. However, these optimization researches are all conducted at single design point and single design objective. As a result, the aerodynamic characteristics of these optimized airfoils still have greater improvement under dynamic stall conditions.

* Corresponding author.
E-mail addresses: mingqingwq@nuaa.edu.cn (Q. Wang), zhaoqijun@nuaa.edu.cn (Q. Zhao).

https://doi.org/10.1016/j.ast.2017.11.033
1270-9638/

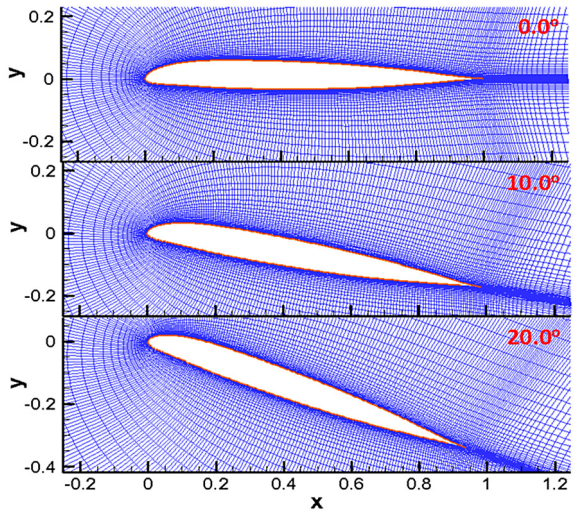

Fig. 1. Sketch of grid deformation.

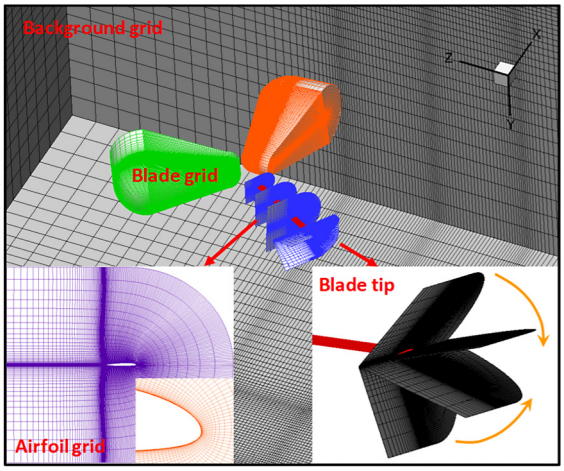

Fig. 2. Sketch of the moving-embedded grids.

Therefore, the purpose of this investigation is to design a new rotor airfoil under dynamic stall conditions using multi-objectives and multi-constraints, and verify the design effectiveness under three-dimensional (3-D) rotor condition. To accomplish this work, a new method is established by coupling the Sequential Quadratic Programming (SQP) method with CFD method, then a new airfoil with better dynamic stall characteristics, i.e. smaller peaks of *Cm* and *Cd*, is optimized based on the OA209 airfoil by employing this optimal method. The URANS equations coupled with the Spalart–Allmaras turbulence model are chosen as the governing equations to simulate the unsteady flowfield of airfoil.

2. Numerical method

2.1. Grid generation method

A C-topology grid around rotor airfoil are generated by solving the Poisson equations [22]. The governing equations of the grid generation (2-D) can be written as

$$\begin{cases} \xi_{xx} + \xi_{yy} = P(\xi, \eta) \\ \eta_{xx} + \eta_{yy} = Q(\xi, \eta) \end{cases} \tag{1}$$

where, the control functions of $P(\xi, \eta)$ and $Q(\xi, \eta)$ determine the skewness and spacing of the grid. The computational domain of the airfoil is consisted of 459×80 points. In order to satisfy the requirements of unsteady aerodynamic characteristics calculation, a deforming grid is employed to simulate the flowfield of rotor airfoil under dynamic stall conditions. Therefore, the geometric conservation law is introduced to avoid the error due to the grid deformation, i.e.

$$\frac{\partial}{\partial t}\int_{\Omega} d\Omega - \iint_{\partial\Omega} \boldsymbol{V}_t \cdot \boldsymbol{n} dS = 0 \tag{2}$$

where, Ω represents the control volume, t represents the physical time, $\boldsymbol{V}_t$ represents the moving velocity of grid edges, S is the face of mesh and $\boldsymbol{n}$ denotes the unit normal vector to the face. The sketch of grid deformation at different angle of attack (AoA) is shown in Fig. 1, and it can be seen that the deforming grids around the airfoil still keep orthogonality well even at AoA $= 20°$.

The 3-D rotor blade grids with C–O topology are generated based on the 2-D airfoil grids for the simulation of rotor under forward flight condition, and the size of the blade grids are 399 (chord-wise) $\times$ 80 (span-wise) $\times$ 60 (normal). To allow the relative motion between components, the moving-embedded grid method is employed in this research, and the size of the background grids is 160 (forward direction) $\times$ 120 (vertical direction) $\times$ 160 (horizontal direction). The hole-boundary is identified by employing the Hole Map method, and the Inverse Map method is used to search the donor element [12]. The sketch of the moving-embedded grids is shown in Fig. 2.

2.2. Numerical method for unsteady flowfield simulation

The integral form of the Navier–Stokes equations is employed to simulate the unsteady compressible flowfield of airfoil and rotor, i.e.

$$\frac{\partial}{\partial t}\int_{\Omega} \boldsymbol{W} d\Omega + \iint_{\partial\Omega} (\boldsymbol{F}_c - \boldsymbol{F}_v) d\boldsymbol{S} = 0 \tag{3}$$

where, $\boldsymbol{W}$ denotes the vector of conserved variables, $\boldsymbol{F}_c$ denotes the vector of convective fluxes, and $\boldsymbol{F}_v$ denotes the vector of viscous fluxes, as follows

$$\boldsymbol{W} = \begin{bmatrix} \rho \\ \rho u \\ \rho v \\ \rho E \end{bmatrix}, \quad \boldsymbol{F}_c = \begin{bmatrix} \rho \boldsymbol{V}_r \\ \rho u \boldsymbol{V}_r + n_x p \\ \rho v \boldsymbol{V}_r + n_y p \\ \rho H \boldsymbol{V}_r + \boldsymbol{V}_t p \end{bmatrix},$$

$$\boldsymbol{F}_v = \begin{bmatrix} 0 \\ n_x \tau_{xx} + n_y \tau_{xy} \\ n_x \tau_{yx} + n_y \tau_{yy} \\ n_x \Theta_x + n_y \Theta_y \end{bmatrix} \tag{4}$$

where, $\boldsymbol{V}_r = \boldsymbol{V} - \boldsymbol{V}_t$, $\boldsymbol{V}$ denotes the absolute velocity, and $\boldsymbol{V}_t$ denotes the contravariant velocity. ρ, E, p and H represent the density, total energy, static pressure and total enthalpy, respectively. τ_{ij} represents the viscous stresses, and Θ_i are terms describing the work of the viscous stresses and the heat condition in the fluid.

Aiming to predict the non-linear and unsteady characteristics of vortical flowfield of rotor, the Roe method [23] coupled with third-order MUSCL scheme [24] is employed for the discretization of convective fluxes. The numerical flux on the cell faces is given by:

$$(\boldsymbol{F}_c)_{i+1/2} = \frac{1}{2}\left[\boldsymbol{F}_c(\boldsymbol{q}_R) + \boldsymbol{F}_c(\boldsymbol{q}_L) - |\bar{\boldsymbol{A}}_{Roe}|_{i+1/2}(\boldsymbol{q}_R - \boldsymbol{q}_L)\right] \tag{5}$$

The product of $|\bar{\boldsymbol{A}}_{Roe}|$ and the difference of the left and right state could be efficiently expressed as: